2018 European Control Conference (ECC)
June 12-15, 2018. Limassol, Cyprus

Topology Control of Networks of Proximity Kuramoto Oscillators

Pietro DeLellis[1], Gianluca Falanga[1], Franco Garofalo[1] and Francesco Lo Iudice[1]

***Abstract*— In this paper, we propose a decentralized strategy to control the topology of Kuramoto oscillators coupled via a proximity rule. In particular, the proposed control law is capable of steering the oscillators' dynamics so that a desired steady-state topology is achieved. This result is obtained through a decentralized and discontinuous feedback control action that relies only on local information available at each node. The effectiveness of the control strategy is demonstrated through extensive numerical simulations.**

I. Introduction

The problem of coordinating the motion of ensembles of dynamical systems has attracted the efforts of several research communities due to its relevance in diverse contexts, as in animal behavior [1], [2], rendezvous problems [3], power grids [4], and multi-vehicle control [5], among the others. For instance, the control of fleets of autonomous vehicles [6] is one of the most relevant challenges in control today due to the ever increasing diffusion of such vehicles. Noticeably, the number of possible applications grows as the price of the technology decreases, and this motivated the scientific community to tackle scenarios in which the agents can communicate only when their distance is lower than a certain threshold, as in fleets of autonomous vehicles equipped with cheap proximity sensors [7]–[10]. If this is the case, the interconnection topology regulating the communication among the agents becomes state-dependent, and the problem arises of selecting the topology the agents should keep in their coordinated motion.

Differently from past work, which focused on mantaining the connectivity of the formation [11], here we tackle what we call the *topology control* problem, that is, that of controlling the formation towards a specific desired topology. Namely, in this paper we focus on a topology control problem in a network of Kuramoto oscillators that is a paradigmatic model of coupled oscillators [12], [13], still studied nowadays due to its flexibility and capability of generating rich dynamics while keeping analytical tractability [14]–[18]. In particular, in [18] it was shown that, when the communication among the agents takes place only if they are in mutual proximity, the so-called topological bifurcation phenomenon emerges, and multiple stable steady-state topologies arise, depending on the initial conditions and on the coupling strength among the oscillators [18], [19]. Motivated by these results, we find this model the ideal testbed for topology control. Here, we propose a discontinuous feedback control law to steer the dynamics of proximity Kuramoto oscillators towards a desired steady-state topology. Noticeably, the proposed strategy is completely decentralized, and is composed by two complementary actions: the first induces the emergence of the missing links, while the second induces the removal of the excess links. After thoroughly explaining the rationale behind the control law, we demonstrate its effectiveness through extensive numerical simulations.

[1] All authors are with the Department of Electrical Engineering and Information Technology, University of Naples, 80125 Naples, Italy pietro.delellis@unina.it, francesco.loiudice2@unina.it, giovanni.falanga@studenti.unina.it, franco.garofalo@unina.it.

II. Network Model

Let us consider an ensemble of N proximity Kuramoto oscillators [18]. The dynamics of the i-th oscillator are given by

$$\dot{\theta}_i(t) = \omega_i + g\sum_{j=1}^{N} a_{ij}(t)\sin(\theta_j(t) - \theta_i(t)), \tag{1}$$

$$\theta_i(0) = \theta_i^0, \tag{2}$$

for $i = 1, \dots, N$, where $\theta_i(t) \in \mathbb{S}^1$ and $\omega_i \in \mathbb{R}$ are the angle and the natural frequency of the i-th oscillator, respectively, $g > 0$ is the coupling gain, and $a_{ij}(t)$ is the element (i, j) of the adjacency matrix $A(t)$ describing the interconnection topology regulating the communication amongst the agents. In our parametrization of $\mathbb{S}^1$, we assume that the angles are measured counterclockwise and that they take value in $[-\pi,\ \pi[$. Furthermore, for notational purposes we shall omit the state-dependency of the elements of the matrix $A(t)$, whose time evolution is regulated by the following equation:

$$a_{ij}(t) = \begin{cases} 1, & \text{if } d_{ij}(t) \leq \theta_{\text{vis}}, \\ 0, & \text{otherwise}, \end{cases} \tag{3}$$

where $\theta_{\text{vis}} < \pi/2$ is the proximity threshold, and $d_{ij}(t)$ is the geodesic distance [20] between $\theta_i(t)$ and $\theta_j(t)$. Equation (3) allows to model, in the framework of the Kuramoto oscillators, the idea that two agents communicate, and thus interact, if and only if they are sufficiently close to each other. This proximity rule determines a time varying symmetric adjacency matrix $A(t)$, and therefore a time varying undirected graph $\mathcal{G}(t)$ describing the network topology. Figure 1 offers a schematic of this rule: an oscillator is in proximity with the one portrayed in Figure 1 if it lies in the arc subtending the angle in orange.

Definition 1: we say that network (1)-(3) asymptotically achieves *phase locking* (or, equivalently, *frequency synchronization*) if

$$\lim_{t\to+\infty} \left|\dot{\theta}_i(t) - \dot{\theta}_j(t)\right| = 0,$$

for all $i, j = 1, \dots, N$.

If frequency synchronization is achieved, then there clearly exists an $\bar{\omega} \in \mathbb{R}$, called the *entrainment frequency*, such that

$$\lim_{t \to +\infty} \dot{\theta}_i(t) = \bar{\omega},$$

for all $i = 1, \dots, N$.

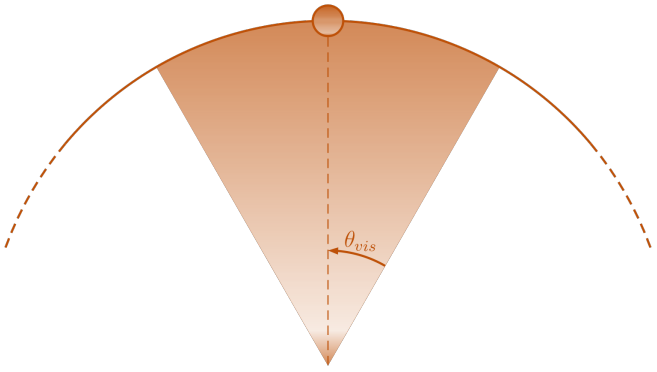

Fig. 1: Schematic of the proximity rule. Any oscillator lying in the the arc subtending the angle highlighted in orange is in proximity with the portrayed oscillator.

Open Loop Dynamics

To introduce our problem formulation and give our main results, we first provide a brief overview of the open loop dynamics of network (1)-(3). We start by noting that, as the agent dynamics are those of the Kuramoto oscillators with heterogeneous natural frequencies ω_i, in principle phase locking could be achieved. If this were the case, then the phase differences $\theta_i(t) - \theta_j(t)$ would converge to a steady state value that is dependent from the specific pair i, j selected. In turn, Equation (3) establishes the existence of a unique graph, which we will call *equilibrium topology*, corresponding to given steady-state phase differences. However, different steady-state configurations may yield to alternative steady-state topologies, and thus the question arises of understanding which graphs can emerge as equilibrium topologies. We emphasize that not all graphs can be equilibrium topologies, as they may not be compatible with model (1)-(3) and Definition 1. Indeed, the equilibrium topology must be consistent with the geodesic distance between the oscillators on the circle. As a trivial example, for $N > 3$ a star graph is not an equilibrium topology.

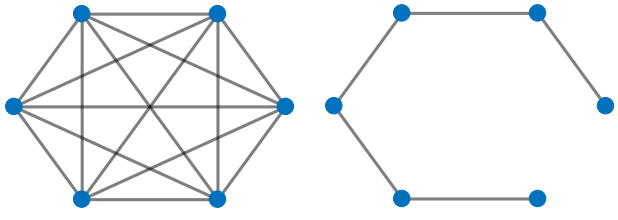

Fig. 2: Schematic of the topologies A_0^1 (a) and A_0^2 (b).

This problem of determining whether a graph can be an equilibrium for the network model (1)-(3) was studied in [18], where some necessary conditions on the adjacency matrix $\bar{A}$ were introduced. Here, we review such conditions as they will be relevant for the comprehension of our control law. First, we note that for an adjacency matrix $\bar{A}$ to be an equilibrium topology, there must exist scalars θ_i, $i = 1, \dots, N$ fulfilling the following set of conditions:

$$\bar{\omega} = \omega_i + g \sum_{j=1}^{N} \bar{a}_{ij} \sin(\theta_j - \theta_i), \quad i = 1, ..., N, \tag{4}$$

$$d_{ij} \leq \theta_{\text{vis}} \qquad i, j \mid \tilde{a}_{ij} = 1 \tag{5}$$

$$d_{ij} > \theta_{\text{vis}} \qquad i, j \mid \tilde{a}_{ij} = 0 \tag{6}$$

Moreover, the entrainment frequency can be computed as in [16]: leveraging the symmetry of the proximity network and the oddness of the sine function, summing Equations (4) for $i = 1, ..., N$ and dividing by N yields

$$\bar{\omega} = \frac{1}{N} \sum_{i=1}^{N} \omega_i. \tag{7}$$

Substituting Equation (7) in (4), one can easily obtain

$$\sum_{j=1}^{N} \bar{a}_{ij} \sin(\theta_j - \theta_i) = \frac{\bar{\omega} - \omega_i}{g} \qquad i = 1, ..., N, \tag{8}$$

which highlights the inverse proportionality between the phase differences and the coupling gain at steady-state. As a consequence, there will be a $\bar{g}$ such that for all coupling gains $g > \bar{g}$ the only feasible equilibrium topology is the all-to-all. However, in [18] it was illustrated that, for values lower than this theoretical threshold $\bar{g}$, Equation (4) can be satisfied for more than one equilibrium topology. This last consideration motivated a numerical analysis which evidentiated a phenomenon called *topological bifurcation* [18], that is, the dependency of the achieved equilibrium topology on the value of the coupling gain g and on the initial conditions of the oscillators. We emphasize that, in absence of a control action, no available theoretical tools can predict the topology that will emerge at steady state for a given set of initial conditions.

To better illustrate the bifurcation phenomenon, we show the results of two numerical simulations of the network (1)-(3) with $N = 6$. The twin simulations share the same selection of natural frequencies ω_i, $i = 1, \dots, 6$, the same coupling gain g, and the same visibility angle θ_{vis}. However, their initial topologies A_0^1 and A_0^2 differ because of a different selection of the initial conditions: in Simulation 1 we select $\theta_i^1(0)$, $i = 1, \dots, N$, such that A_0^1 defines the all-to-all graph sketched in Fig. 2(a), while in Simulation 2 we select $\theta_i^2(0)$, $i = 1, \dots, N$, so that A_0^2 defines the chain topology sketched in Fig. 2(b). As shown in Figs. 3 and 4, despite the simulation parameters being the same, the difference in the initial conditions yields a substantial difference in the phase locked state, coherently with the observation that in both simulations the achieved equilibrium topology $\bar{A}$ is identical to the initial topology, that is $\bar{A} = A_0^i$, $i = 1, 2$. Specifically,

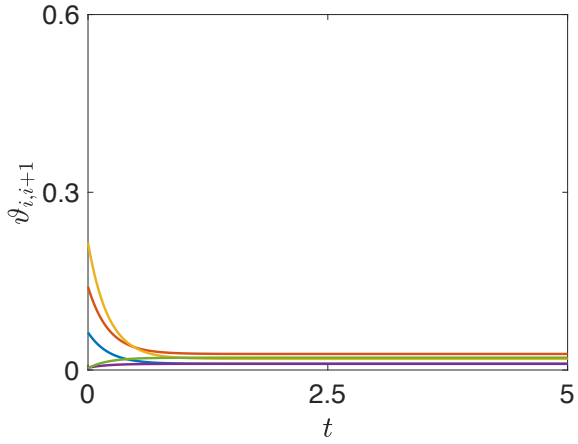

Fig. 3: Simulation 1: open loop dynamics, $A(0) = A_0^1$. Plot of the time evolution of the phase differences of consecutive oscillators.

as the reader may notice, in Simulation 1 $\bar{A}$ is the most dense topology, while in Simulation 2 it is the sparsest connected topology, which reflects into a noticeably different steady-state.

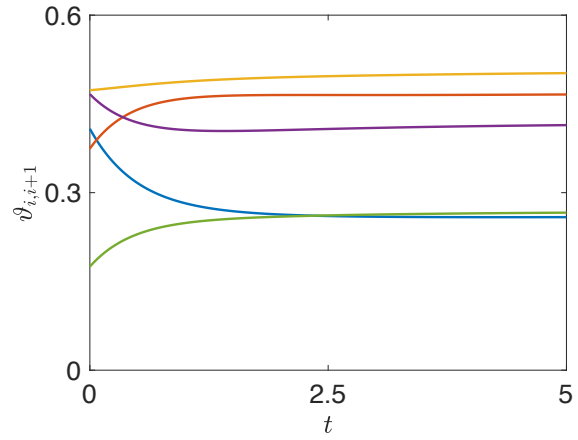

Fig. 4: Simulation 2: open loop dynamics, $A(0) = A_0^2$. Plot of the time evolution of the phase differences of consecutive oscillators.

III. Decentralized Control Startegy

When controlled, the dynamics of the i-th proximity Kuramoto oscillator becomes

$$\dot{\theta}_i(t) = \omega_i + g\sum_{j=1}^{N} a_{ij}(t)\sin(\theta_j(t) - \theta_i(t)) + u_i(t), \quad (9)$$

for all $i = 1, \dots, N$.

Definition 2: The controlled proximity Kuramoto oscillators network (2), (3), (9) asymptotically converges towards an equilibrium topology $\bar{\mathcal{G}}$ with associated adjacency matrix $\bar{A}$ if phase locking is achieved and

$$\lim_{t\to+\infty} a_{ij}(t) = \begin{cases} 0, & \text{if } \bar{a}_{ij} = 0, \\ 1, & \text{if } \bar{a}_{ij} = 1, \end{cases}$$

where $\bar{a}_{ij}$ is the (i,j)-th element of $\bar{A}$.

Our control objective is to design a decentralized feedback control action u_i to ensure that the proximity Kuramoto oscillators asymptotically converge towards a desired equilibrium topology $\tilde{\mathcal{G}}$.

Control Law

To achieve our goal, we propose the following distributed and discontinuous control action:

$$u_i(t) = \mathcal{I}_{\mathbb{R}+}\left(\tilde{k}_i - k_i(t)\right) g\delta \sum_{j=1}^{N} \tilde{a}_{ij} a_{ij}(t)\sin\left(\theta_j(t) - \theta_i(t)\right) + g\sum_{j=1}^{N}(1-\tilde{a}_{ij})a_{ij}(t)\sin(\theta_i(t) - \theta_j(t)), \quad (10)$$

where $\tilde{k}_i := \sum_j \tilde{a}_{ij}$ and $k_i(t) := \sum_j a_{ij}(t)$ are the desired and current degree of oscillator i, respectively, and δ is a tunable control parameter. The rationale behind the two additive terms in (10) is the following:

- The first term is an attractive force that activates only when the desired degree is lower than the current degree of node i, and only between agents that at steady state must be directly connected. The higher the number of missing links to achieve, the higher the gain is, the higher the attractive term will be. The indicator function $\mathcal{I}_{\mathbb{R}+}(\cdot)$ ensures the forces are always attractive and never repulsive.
- The second term is instead a repulsive force that activates only when there are edges in the current topology $\mathcal{G}$ that are not present in the desired equilibrium topology $\tilde{\mathcal{G}}$. Namely, for a given node i, the second control action activates if there exists a node $j \neq i$ such that $a_{ij}(t) = 1$ and $\tilde{a}_{ij} = 0$.

Summing up, the designed control law aims at eliminating the multiplicity of equilibria that characterize the dynamics of network (1) by neutralizing the effect of undesired edges, that is, edges of $\mathcal{G}(t)$ that do not appear in $\tilde{\mathcal{G}}$, and by introducing additional attractive forces that allow increasing the current network connectivity in order to achieve a denser equilibrium topology. Conversely, as $u(t) = 0$ when $A(t) = \tilde{A}$, our control law does not preclude $\tilde{\mathcal{G}}$ be an equilibrium topology for the uncontrolled dynamics.

We emphasize that the proposed control law is completely decentralized. Indeed, node i needs to access only local information, such as its current and desired degree ($k_i(t)$ and $\tilde{k}_i$, respectively), and the current and desired connections to be activated with its neighbors (given by the values $a_{ij}(t)$ and $\tilde{a}_{ij}$, $j = 1, \dots, N$, respectively).

As our control law was designed to eliminate the multiplicity of equilibria that characterize the open loop dynamics, in the next section, we will investigate its ability to do so and the possible emergence of new equilibria which could preclude the effectiveness of our control action.

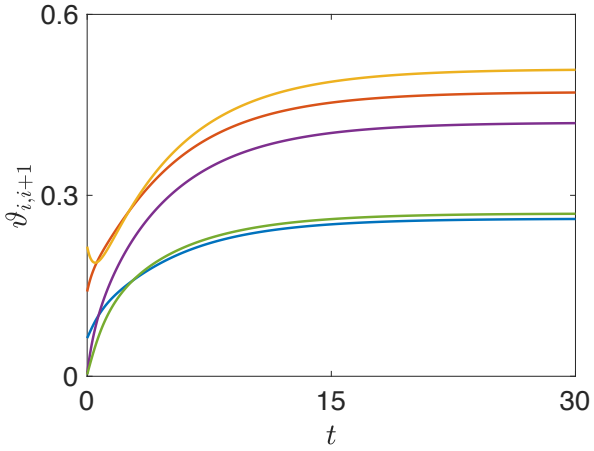

Fig. 5: Simulation 3: closed loop dynamcis, $A(0) = A_0^1$. Plot of the time evolution of the phase differences of consecutive oscillators.

IV. Results

We start by showcasing the results of two simulations (hereafter named Simulation 3 and 4, respectively) of the closed loop dynamics, conducted to highlight the differences with the open loop dynamics. In particular Simulation 3 (4) shares the same initial conditions and parameters of Simulation 1 (2). Therefore, the initial topology in Simulation 3 will be A_0^1 (the all-to-all) while the initial topology in Simulation 4 will be A_0^2 (the chain). The control goal in Simulation 3 (4) will be to drive the network topology away from the all-to-all (chain) to achieve at steady state the chain (all-to-all), as summarized in Table I. By inspecting

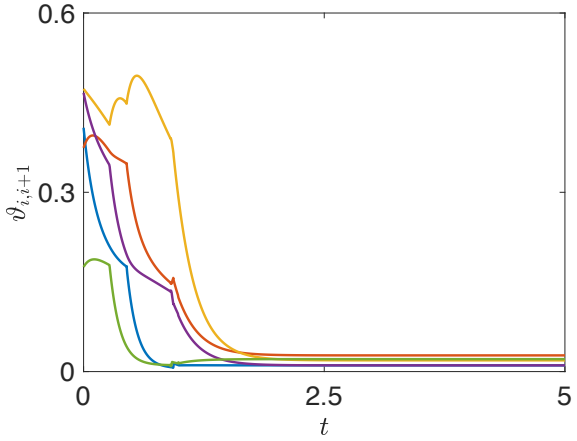

Fig. 6: Simulation 4: closed loop dynamcis, $A(0) = A_0^2$. Plot of the time evolution of the phase differences of consecutive oscillators.

Fig. 5, we can observe that in Simulation 3, although the initial topology $A(0)$ is the all-to-all and thus each agent can initially communicate with all the others, the repulsive forces neutralize the effect of the undesired edges: this ensures the agents appropriately space and reach the desired chain topology instead of the equilibrium associated to the all-to-all configuration achieved in Simulation 1, see Fig. 3. The opposite happens in Simulation 4, where the attractive forces determined by the sparsity of $A(0)$ make sure the agents get closer. Thanks to such effect denser and denser topologies appear (the transition between the topologies reflects in a discontinuity in the time evolution of $\theta_{i,i+1}$ that can be distinctly noted in Fig. 6) until the all-to-all configuration is finally achieved.

TABLE I: Initial and final topologies for the Simulations 1-4. OL and CL stand for open and closed loop, respectively.

Simulation	OL vs CL	$\mathbf{A(0)}$	$\bar{\mathbf{A}}$	$\tilde{\mathbf{A}}$
1	OL	A_0^1	A_0^1	-
2	OL	A_0^2	A_0^2	-
3	CL	A_0^1	A_0^2	A_0^2
4	CL	A_0^2	A_0^1	A_0^1

While the previous results suggest that the decentralized control strategy (10) can succeed in eliminating the undesired equilibria exhibited by the open loop dynamics, it remains to be proven if undesired additional equilibria in which the closed loop network may get trapped can arise. To study the possible emergence of new undesired equilibria, we start by distinguishing between two cases, (a) that in which phase locking arises in a disconnected topology, and (b) that in which phase locking arises in a connected topology. As for case (a), phase locking in a disconnected topology should arise only for a set of Lebesgue measure zero of the agents' natural frequencies ω_i. Indeed, if phase locking arises, we then have that

$$\dot{\theta} = 1_N \bar{\omega} \tag{11}$$

where θ is the stack vector of all the angular positions of the agents, and 1_N is the N-dimensional column vector with all entries equal to one. Eq. (11) implies that each angular difference $\theta_{ij}(t)$ reaches a constant value $\bar{\theta}_{ij}$. Now, if the agents synchronize in a connected topology, then each $\dot{\theta}_i$ depends either directly or indirectly on all the angular differences θ_{ij} and all the natural frequencies ω_i. Hence, if we perform an infinitesimal variation $d\omega_i$ of a natural frequency ω_i this should reflect into a perturbation of the phase locked state. Namely, $d\omega_i$ should translate into a variation $d\bar{\theta}_{ij}$ of the steady state angular differences $\bar{\theta}_{ij}$ and in turn of the common angular velocity $\bar{\omega}$ of all the agents unless $d\bar{\theta}_{ij}$ is able to determine a variation of the network topology thus breaking the phase locked state. On the other hand, if the agents phase lock in a disconnected topology of m clusters, a variation $d\omega_i$ of a natural frequency ω_i does not yield a variation of the common angular velocity of all the agents, but only of the oscillators of the cluster to which i belongs to. Hence, $d\omega_i$ would generate a difference in the oscillators angular velocities thus breaking the phase-locked state.

While equilibria in disconnected equilibrium topologies should only arise for a set of Lebesgue measure zero of

the network parameters, excluding the emergence of new equilibra in a connected topology is nontrivial. Therefore, in what follows we perform an extensive numerical campaign to study the possible emergence of such equlibria, and to test the possibility of eliminating them by appropriately tuning the control parameter δ, thus validating the effectiveness of our control strategy. Specifically, we consider a network of $N = 6$ Kuramoto oscillators characterized by the following natural frequencies:

$$\omega = [0.18\ 0.23\ 0.36\ 0.45\ 0.50\ 0.60].$$

Moreover, we select $\theta_{\text{vis}} = \pi/N$ and perform $Q = 10000$ numerical simulations with random initial conditions for each of three different desired equilibrium topologies $\tilde{A}_1$, $\tilde{A}_2$, and $\tilde{A}_3$. Namely, we select $\tilde{A}_1 = A_0^1$ (all-to-all), $\tilde{A}_2 = A_0^2$ (chain), and $\tilde{A}_3$ as the topology depicted in Fig. 7. Indeed, as $\tilde{A}_1$ only activates the attractive forces in eq. (10), while $\tilde{A}_2$ only the repulsive ones, we introduced $\tilde{A}_3$ to consider the cases in which both terms of the control law (10) can be simultaneously active. For each simulation conducted with $\tilde{A} = \tilde{A}_1$ or $\tilde{A} = \tilde{A}_3$ we select $g = 0.4$, while for each simulation conducted with $\tilde{A} = A_2$, the sparsest desired topology, we select $g = 0.9$, while δ was initially set to the value of 1 for all the $3Q$ simulations

First, we ran each numerical simulation for $T = 200$ time instants and found that the desired equilibrium topology was always achieved for $\tilde{A} = \tilde{A}_2$. Instead, when $\tilde{A} = \tilde{A}_1$ or $\tilde{A} = \tilde{A}_3$ the network got trapped into several equilibrium topologies sparser than $\tilde{A}$. This spurred us to increase δ to the value of 2 to strengthen the attractive forces. Running again the entire set of numerical simulations for $\delta = 2$, we found that the desired equilibrium topology was always achieved for $\tilde{A} = A_2$ and $\tilde{A} = \tilde{A}_3$ while for $\tilde{A} = \tilde{A}_1$, in approximately the 6% of the simulations phase locking was not achieved and two disconnected clusters of synchronized agents arose. However, these clusters were characterized by slightly different angular velocities and thus eventually came in proximity of each other as we increased T, thus successfully achieving phase locking in the desired topology $\tilde{A}_1$. Hence, overall, our extensive campaign provides strong numerical evidence supporting our conjecture that the proposed control strategy succeeds achieving topology control. Specifically, we always found a value of the control parameter δ capable of canceling all the undesired equilibria. Moreover, we found numerical evidence supporting our conjecture that phase-locking in a disconnected topology can only be achieved for a set of Lebesgue measure zero of the natural frequencies $\omega_i\ \forall i$, as any time a disconnected topology of m synchronized clusters arose during a numerical experiment, they asymptotically merged into a unique cluster.

V. Conclusions

In this paper we tackled the problem of controlling a network of Kuramoto oscillators coupled through a proximity rule. As this coupling protocol determines the state-dependency of the network topology, our control goal was that of locking the phase of the agents in a desired steady state configuration corresponding to a target adjacency matrix $\tilde{A}$. To solve what we termed the topology control problem, we had to tackle two separate challenges, that is, (i) the problem of guaranteeing the existence of the desired equilibrium in the closed-loop dynamics, and (ii) the problem of extending its basin of attraction by making the desired topology attractive if starting from any other initial topology. As the state-dependency of our network is due to a proximity rule, we tackled these challenges it by introducing in our control law both attractive and repulsive forces between the agents with so as to modify the sparsity of the network topology at will. Specifically, we devised a decentralized discontinuous feedback control law to eliminate the multiplicity of equilibria exhibited by the open loop network dynamics thus allowing to achieve synchronization towards the desired equilibrium topology $\tilde{A}$. The effectiveness of the strategy was illustrated through extensive numerical simulations that showed that it was always possible to tune a control parameter so as to achieve the desired topology. The encouraging numerical results showcased in this work represent a goad to unravel open theoretical and applicative questions in topology control of agents coupled through proximity rules. A first challenging task is to find analytical conditions on the interval of gains g and δ guaranteeing the achievement of a desired topology when the agents are Kuramoto oscillators. Afterwards, the current framework could be extended to the case of agents moving in a two or three dimensional space thus getting closer to the several applicative scenarios, as for instance formation control problems of unmanned vehicles equipped with low-cost proximity sensors.

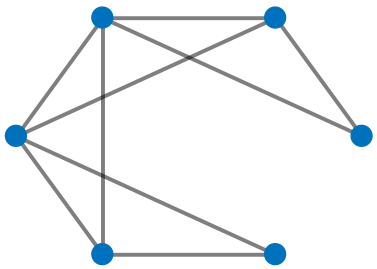

Fig. 7: Schematic of the topology $\tilde{A}_3$.

References

[1] J. H. Fewell, "Social insect networks," *Science*, vol. 301, pp. 1867–1870, 2003.

[2] P. DeLellis, G. Polverino, G. Ustuner, N. Abaid, S. Macri, E. M. Bollt, and M. Porfiri, "Collective behaviour across animal species," *Scientific Reports*, vol. 4, no. 3723, 2014.

[3] J. Cortes, S. Martinez, and F. Bullo, "Robust rendezvous for mobile autonomous agents via proximity graphs in arbitrary dimensions," *IEEE Transactions on Automatic Control*, vol. 51, pp. 1289–1298, 2006.

[4] F. Dorfler and F. Bullo, "Synchronization and transient stability in power networks and nonuniform kuramoto oscillators," *SIAM Journal on Control and Optimization*, vol. 50, no. 3, pp. 1616–1642, 2012.

[5] W. Ren and R. W. Beard, *Distributed Consensus in Multi-vehicle Cooperative Control*. Springer, 2008.
[6] A. Jadbabaie, J. Lin, and A. S. Morse, "Coordination of groups of mobile autonomous agents using nearest neighbor rules," *IEEE Transactions on Automatic Control*, vol. 48, no. 6, pp. 988–1001, 2003.
[7] M. Gauci, J. Chen, T. J. Dodd, and R. Groß, *Distributed autonomous robotic systems*. Springer, Berlin, Heidelberg., 2014, ch. Evolving aggregation behaviors in multi-robot systems with binary sensors, pp. 355–367.
[8] D. Jeong, M. Cho, O. Gnawali, and H. Lee, "Proactive patrol dispatch surveillance system by inferring mobile trajectories of multiple intruders using binary proximity sensors," in *The 35th Annual IEEE International Conference on Computer Communications, IEEE INFOCOM 2016*, 2016, pp. 1–9.
[9] P. DeLellis, F. Garofalo, F. Lo Iudice, and G. Mancini, "State estimation of heterogeneous oscillators by means of proximity measurements," *Automatica*, vol. 51, no. 1, pp. 378–384, 2015.
[10] ——, "Decentralized coordination of a multi-agent systembased on intermittent data," *International Journal of Control*, vol. 88, no. 8, pp. 1–16, 2015.
[11] M. M. Zavlanos and G. J. Pappas, "Distributed connectivity control of mobile networks," *IEEE Transactions on Robotics*, vol. 24, no. 6, pp. 1416–1428, 2008.
[12] Y. Kuramoto, "Self-entrainment of a population of coupled non-linear oscillators," in *International Symposium on Mathematical Problems in Theoretical Physics*. Springer, 1975, pp. 420–422.
[13] ——, *Chemical oscillations, waves, and turbulence*, Springer, Ed. Berlin, NY: Springer Verlag, 1984.
[14] F. Dorfler and F. Bullo, "Topological equivalence of a structure-preserving power network model and a non-uniform kuramoto model of coupled oscillators," in *50th IEEE Conference on Decision and Control and European Control Conference (CDC-ECC)*, Orlando, FL, 2011, pp. 7099–7104.
[15] T. Coletta, R. Delabays, and P. Jacquod, "Finite-size scaling in the kuramoto model," *Physical Review E*, vol. 95, no. 4, p. 042207, 2017.
[16] F. Radicchi and H. Meyer-Ortmanns, "Reentrant synchronization and pattern formation in pacemaker-entrained kuramoto oscillators," *Physical Review E*, vol. 74, no. 2, p. 026203, 2006.
[17] H. Hong, K. P. O'Keeffe, and S. H. Strogatz, "Correlated disorder in the kuramoto model: Effects on phase coherence, finite-size scaling, and dynamic fluctuations," *Chaos*, 2016.
[18] P. DeLellis, F. Garofalo, F. Lo Iudice, and G. Pugliese Carratelli, "Topological bifurcations in networks of proximity kuramoto oscillators," in *2015 IEEE International Symposium on Circuits and Systems*, Lisbon, Portugal, 2015, pp. 2688–2691.
[19] T. E. Gorochowski, M. di Bernardo, and C. S. Grierson, "Evolving enhanced topologies for the synchronization of dynamical complex networks," *Physical Review E*, vol. 81, no. 5, p. 056212, 2010.
[20] F. Bullo, *Lectures on network systems*. Version 0.96, 2016.